

Influence of Fluoride Concentration and pH Value on the Corrosion Behaviour of Iron

Ivana Mišković* and Zora Pilić

University of Mostar, Faculty of Science and Education, Department of Chemistry, Matice Hrvatske bb, 88 000 Mostar, Bosnia and Herzegovina

*E-mail: ivana.miskovic@sve-mo.ba

Received: 26 April 2013 / Accepted: 15 May 2013 / Published: 1 June 2013

The growth kinetics and electrochemical properties of the oxide film formed on iron were studied in 0.01 and 0.1 mol L⁻¹ NaF solutions with different pH values (4.5, 5.5 and 6.5) by cyclic voltammetry and electrochemical impedance spectroscopy. The growth of the oxide film on iron in potentiodynamic conditions, characterized by the occurrence of "current plateau" recorded on the cyclic voltammograms, showed that the growth of the oxide film takes place by low-field migration mechanism. The ionic conductivity of the oxide during its growth ($\sim 10^{-12}$ S cm⁻¹) and the electric field strength through the oxide ($\sim 10^6$ V cm⁻¹) were calculated. Thickness of oxide film is dependent upon the solution pH and fluoride concentration; thinner and more compact film forms in solution with lower fluoride concentrations and higher pH values. Impedance measurements were carried out on the potentiostatically formed oxide films after electrode stabilization for 30 minutes at the open circuit potential (E_{OCP}). The charge transfer resistance and the electrode capacitance were determined. The resistance value, as well as E_{OCP} value, decreases with increasing concentration of F⁻ and lowering the pH. Corrosion rate values were computed from charge transfer resistance and it was found that corrosion rate increased with increased F⁻ concentration and decreased pH, being highest in 0.1 mol L⁻¹ NaF, pH=4.5 (60.69 $\mu\text{g cm}^{-2} \text{h}^{-1}$) and lowest in 0.01 mol L⁻¹ pH=6.5 (0.25 $\mu\text{g cm}^{-2} \text{h}^{-1}$).

Keywords: Iron, Passive film, Fluoride ions, Cyclic voltammetry, Electrochemical impedance spectroscopy

1. INTRODUCTION

The properties of iron passive films are of great technological importance because iron is widely used as construction material in processing industry. The dissolution of iron in aqueous solutions have been extensively studied and now is commonly accepted [1,2] that the initial step in active dissolution is rapid chemical dissociation of water molecules by the metal surface to form a

surface compound $[\text{FeOH}]_{\text{ads}}^-$ which is converted into adsorbed $\text{Fe(OH)}_{\text{ads}}$ following an electron transfer. According to the catalytic mechanism, $\text{Fe(OH)}_{\text{ads}}$ enters in a catalytic sequence of dissolution at the end of which $\text{Fe(OH)}_{\text{ads}}$ is regenerated and Fe dissolved as $(\text{FeOH})^+$. According to the consecutive mechanism, $\text{Fe(OH)}_{\text{ads}}$ enters in a noncatalytic one-electron transfer step by which it is oxidized to $(\text{FeOH})^+$. Both mechanism involves the final conversion of $(\text{FeOH})^+$ to stable $\text{Fe}_{\text{aq}}^{2+}$ by $\text{H}_{\text{aq}}^{2+}$. When the current or potential exceeds a certain limit, accumulation and further oxidation of $\text{Fe(II)}_{\text{ads}}$ on the electrode surface leads to formation of a thin protective layer of the $\gamma\text{-Fe}_2\text{O}_3/\text{Fe}_3\text{O}_4$ type [1, 2] hence passivation. The composition of the passive film on iron depends on the type of electrochemical treatment for forming the film and the nature of the solution in which it is formed. Nagayama and Cohen [3, 4], using the electron diffraction method, have shown that the passive film on iron is a duplex layer which is composed of a Fe_3O_4 inner layer and $\gamma\text{-Fe}_2\text{O}_3$ outer layer and the data obtained by surface analytical techniques in general support that duplex, cubic oxide structure [5-8].

The stability of a passive film on iron depends on a large numbers of variables, such as temperature, the chemical composition and the pH of the electrolyte. In the presence of aggressive ions, such as halogenide ions, the passive film on iron may breakdown [9, 10]. The aim of this work is to give more information about influence of fluoride concentration and pH value on the electrochemical behavior of iron. Breakdown of passivity of iron by fluoride occurs in weakly acidic and alkaline solution and generally in strongly acidic solutions [9].

The paper investigates the influence of fluoride concentration and pH value on the kinetics of growth and the electrochemical properties of the surface oxide layer on the iron in 0.01 and 0.1 mol L^{-1} NaF solutions with pH ranging from 4.5 to 6.5. The electrochemical study was performed using the electrochemical techniques of cyclic voltammetry (CV) and electrochemical impedance spectroscopy (EIS).

2. EXPERIMENTAL

2.1. Materials and solutions

Aqueous solutions of 0.01 and 0.1 mol L^{-1} NaF were prepared from NaF (Analytika Ltd., *r.g.*) and ultrapure water. The pH of the solutions (pH 4.5, 5.5 and 6.5) was adjusted by the addition of the appropriate amount of 40% HF (Riedel – de Haen, *p.a.*). The addition of 40% HF had no significant influence on fluoride concentration of working solutions.

Spectroscopically pure iron was used as working electrode. The electrode surface area of 1.327 cm^2 was mechanically abraded by 1200 grade emery paper, degreased with ethanol in an ultrasonic bath and rinsed with ultrapure water before electrochemical measurements.

2.2 Electrochemical measurements

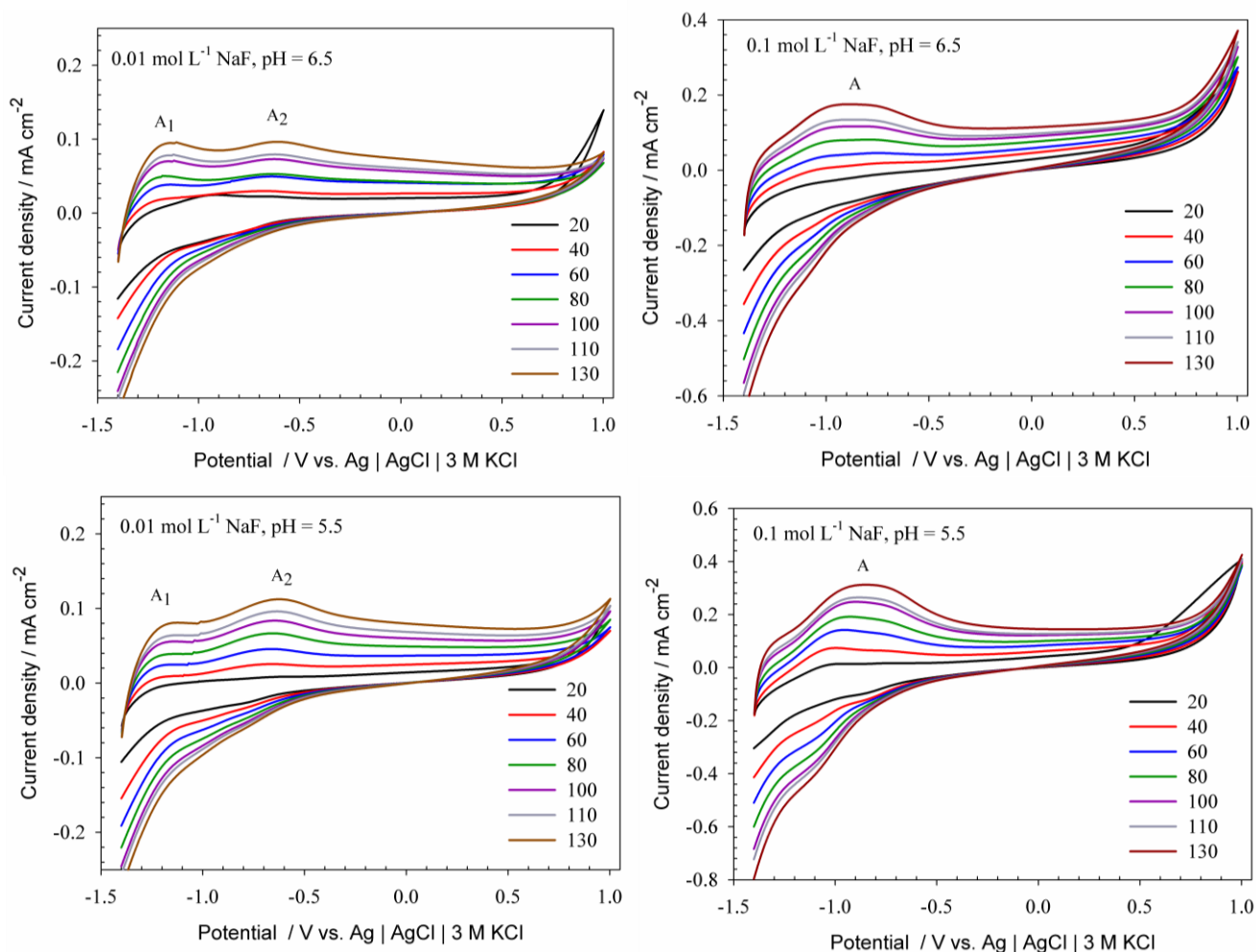
The electrochemical measurements were performed at room temperature in a standard three electrode cell. The counter electrode was a platinum electrode and the reference electrode, to which all

potentials in the paper are referred, was an Ag|AgCl|3 M KCl. All working solutions were deaerated with argon (99,99%) for 30 min prior to each experiment. All electrochemical measurements were performed with an Autolab PGSTAT320N controlled by personal computer using *Nova 1.5*. Cyclic voltammetry measurements were performed in the potential range between -1.4 and 1.0 V, with a scan rates from 20 to 130 mV s^{-1} . Stability of anodic oxide films on iron was examined by continuous cycling (10 cycles) with scan rate 130 mV s^{-1} . EIS measurements were performed in the frequency range between 10000 Hz and 5 mHz with ac potential perturbation of 10 mV amplitude at the open circuit potential. Prior to each measurement the electrode were stabilized for 30 min at the open circuit potential. These procedures gave good reproducibility of results.

3. RESULTS AND DISCUSSION

3.1. Cyclic voltammetry

The cyclic voltamograms recorded for iron in 0.01 mol L^{-1} NaF (pH 4.5, 5.5 and 6.5) and 0.1 mol L^{-1} NaF (pH 4.5, 5.5 and 6.5) solutions, with a increasing scan rates from 20 to 130 mV s^{-1} , are presented in Fig. 1.



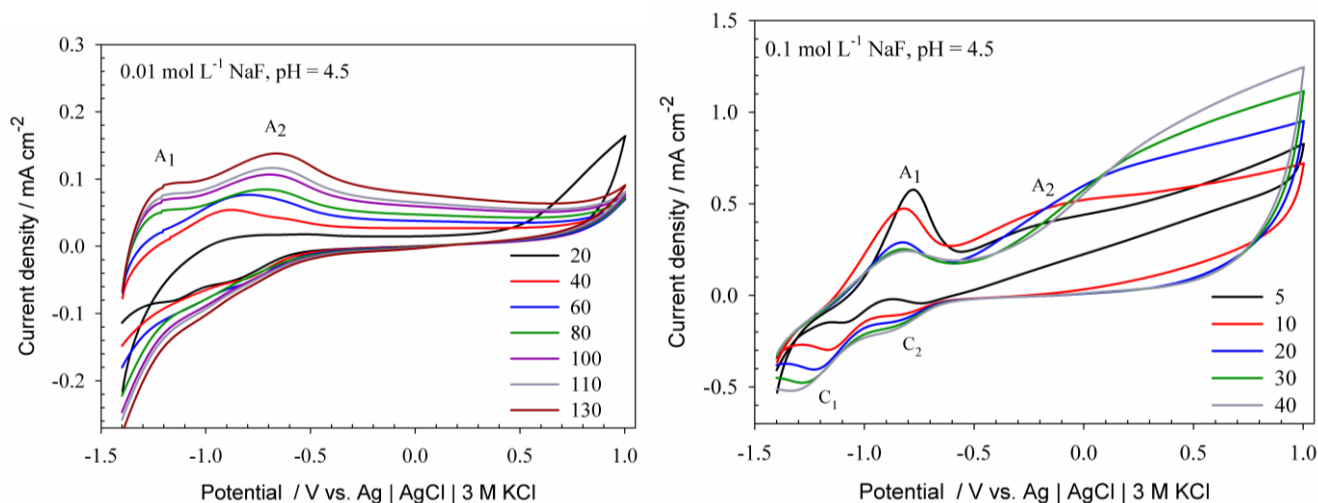


Figure 1. Cyclic voltammograms for iron in 0.01 and 0.1 mol L⁻¹ NaF, pH = 6.5, 5.5 and 4.5 obtained with a increasing scan rates (shown in figure, in mV s⁻¹).

During the anodic sweep the current profile shows two anodic peaks in 0.01 mol L⁻¹ NaF solutions that are shifted towards higher current densities with increasing scan rate. The first oxidation peak, A₁, at -1.1 V, corresponds to the active-passive transition and can be ascribed to the formation of a non-protective Fe(OH)₂ layer [11]. Another peak in the anodic cycle A₂, at -0.6 V in the prepassive region, can be ascribed to the formation of a dense and compact Fe(III) oxide. In the 0.1 mol L⁻¹ NaF solutions (pH = 5.5 and 6.5), only one broad oxidation peak, A can be observed. According to its shape, it seems that current peak A represents two overlapping current peaks. The first one can be ascribed to the formation of Fe(II) species, while the second oxidation peak can be attributed to the Fe(III) oxide formation. In 0.01 mol L⁻¹ NaF (pH 4.5, 5.5 and 6.5) and 0.1 mol L⁻¹ NaF (pH 5.5 and 6.5), at potentials more positive than -0.4 V, current profile reaches a steady-state value (j_{pl}) that remains constant up to ~ 0.9 V. This is passive region where oxide film is thickening with increasing anodic potential [12, 13]. The increase in the current near the potential 0.9 V is due to oxygen evolution. In the 0.1 mol L⁻¹ NaF solution, pH = 4.5, two anodic peaks are observed, but passive region is not established. The electroreduction scan shows well defined current peaks C₂ and C₁ only in 0.1 mol L⁻¹ NaF, pH = 4.5 that are shifted towards higher current densities and more negative potentials with increasing scan rate. They are related to the electroreduction of Fe(III) to Fe(II) and Fe(II) to Fe(0), respectively.

3.1.1 Formation and growth of the anodic film

To investigate mechanism of film formation, cyclic voltammograms from Fig.1 were used. In the potential range from -0.4 V to 0.9 V, currents are practically constant (j_{pl}), indicating steady state film growth in the passive region. The obtained j_{pl}/E response in the potential range from -0.4 V to 0.9 V pointed to a low-field migration mechanism of film growth:

$$j_{pl} = 2AB \times H \quad (1)$$

where j_{pl} is the ionic current density for anodic oxide growth, H is the electric field within the oxide, and AB is ionic conductivity of the oxide layer during its growth.

Linear dependence of steady-state current density (j_{pl}) on the square root of scan rate ($v^{1/2}$), shown in the Fig. 2, justify the application of low-field migration mechanism by the equation [14 - 16]:

$$j_{pl} = \left(\frac{2 z F A B}{V_m} \right)^{1/2} v^{1/2} \tag{2}$$

where V_m , is the molar volume of the growing phase (for Fe_2O_3 , $V_m = 30,47 \text{ cm}^3 \text{ mol}^{-1}$).

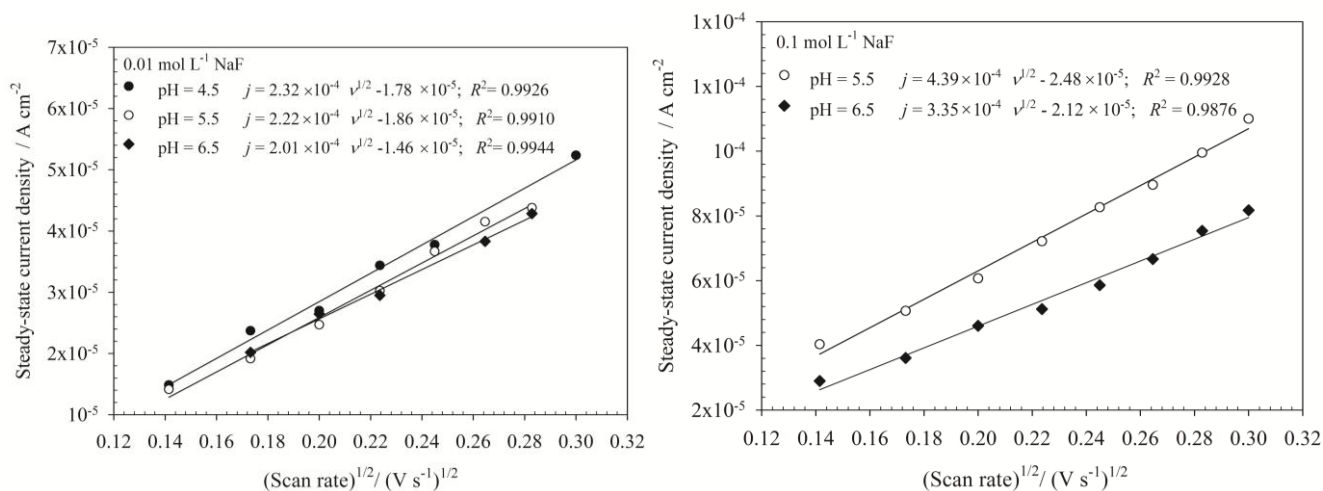


Figure 2. Dependence of the steady-state current density on the square root of the scan rate for iron in 0.01 and 0.1 mol L⁻¹ NaF, pH = 4.5, 5.5 and 6.5.

The values of ionic conductivity of the oxide during its growth (AB) were determined from the slopes of dependences shown in Fig. 2 and presented in Table 1. The values of electric field strength were calculated according to equation (1), using values of j_{pl} from cyclic voltammograms recorded with scan rate 20 mV s⁻¹ (from Fig. 1, given in Table 1) and also presented in Table 1.

Table 1. The kinetic parameters of oxide film growth on iron in NaF solutions.

c (NaF) / mol L ⁻¹	pH	j_{pl} / mA cm ⁻²	(AB) / S cm ⁻¹	H / V cm ⁻¹
0.01	6.5	0.0202	1.06×10^{-12}	9.53×10^6
	5.5	0.0192	1.30×10^{-12}	7.38×10^6
	4.5	0.0237	1.41×10^{-12}	8.40×10^6
0.1	6.5	0.0361	2.95×10^{-12}	6.12×10^6
	5.5	0.0506	5.07×10^{-12}	4.99×10^6
	4.5	-	-	-

The obtained values of the electric field strength (10^6 V cm^{-1}) are in good agreement with the literature [17 - 23].

The total charge of the anodic processes, Q_A are determined by integration of the anodic portions of cyclic voltammograms. Under assumption that the surface layer is mostly composed of Fe_2O_3 oxide [10, 19, 24], its thickness, d was calculated from the anodic charge, Q_A , corresponding to the surface layer oxidation according to the expression:

$$d = \left(\frac{M}{\rho z F} \right) \frac{Q_A}{\sigma} \tag{3}$$

where M is the molar mass of Fe_2O_3 ($M = 159.68 \text{ g mol}^{-1}$), ρ is density of Fe_2O_3 ($\rho = 5.24 \text{ g cm}^{-3}$) [25], z is the number of electrons, F is the Faraday constant and σ is the roughness factor of the surface ($\sigma = 2$).

Table 2. Charge of the anodic processes and thickness of the oxide film in NaF solutions.

c (NaF) / mol L ⁻¹	pH	Q_A / mC cm ⁻²	d / nm
0.01	6.5	5.194	1.367
	5.5	6.416	1.687
	4.5	17.140	4.511
0.1	6.5	11.593	3.051
	5.5	25.927	6.824
	4.5	151.646	39.912

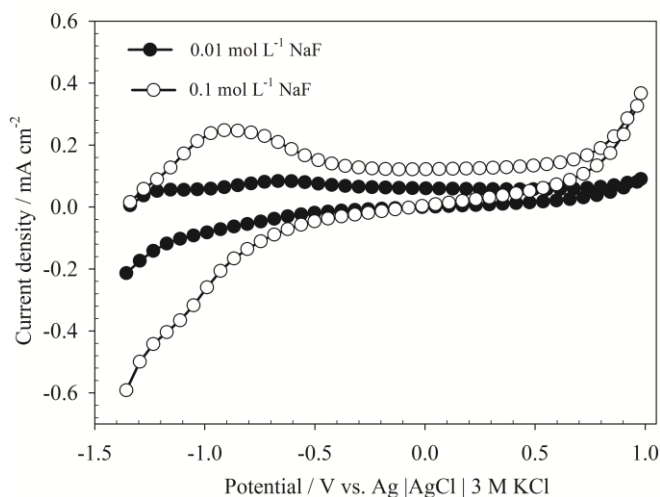


Figure 3. Cyclic voltammograms of iron in 0.01 and 0.1 mol L⁻¹ NaF solutions, pH 6.5, $\nu = 100 \text{ mV s}^{-1}$.

It is clear that the thickness of the passive film increases with increasing F^- concentration and decreasing pH value. At higher pH values and lower F^- concentration, surface layer is thinner with better protective properties [10, 11, 24, 26, 27]. Very high value of oxide thickness in 0.1 mol L⁻¹ NaF,

pH = 4.5 indicates that surface layer is hidratized with no protective properties. The influence of the electrolyte composition on the iron dissolution/passivation process is well illustrated by the cyclic voltammograms shown on Fig. 3 and 4. Fig. 3. shows compared cyclic voltammograms of iron in 0.01 and 0.1 mol L⁻¹ NaF solutions, both at pH 6.5. The current densities are lower in 0.01 mol L⁻¹ than in 0.1 mol L⁻¹ NaF solution and the extent of the passive range slightly increased with the decreasing fluoride concentration. Cyclic voltammograms of iron in 0.01 and 0.1 mol L⁻¹ NaF solutions, with different pH values are compared and shown in Fig. 4. The current densities of anodic peaks indicate that the oxide dissolution is lower at pH 6.5 than at pH 4.5. This is especially expressed in 0.1 mol L⁻¹ NaF where iron cannot establish passive range for pH = 4.5. Stability of anodic passive film on iron was investigated by continuous cycling of electrode with the same scan rate, $\nu = 130 \text{ mV s}^{-1}$ (Fig. 5). With increasing number of cycles, current densities of anodic peaks are lower, while no changes in current densities of cathodic peaks can be observed.

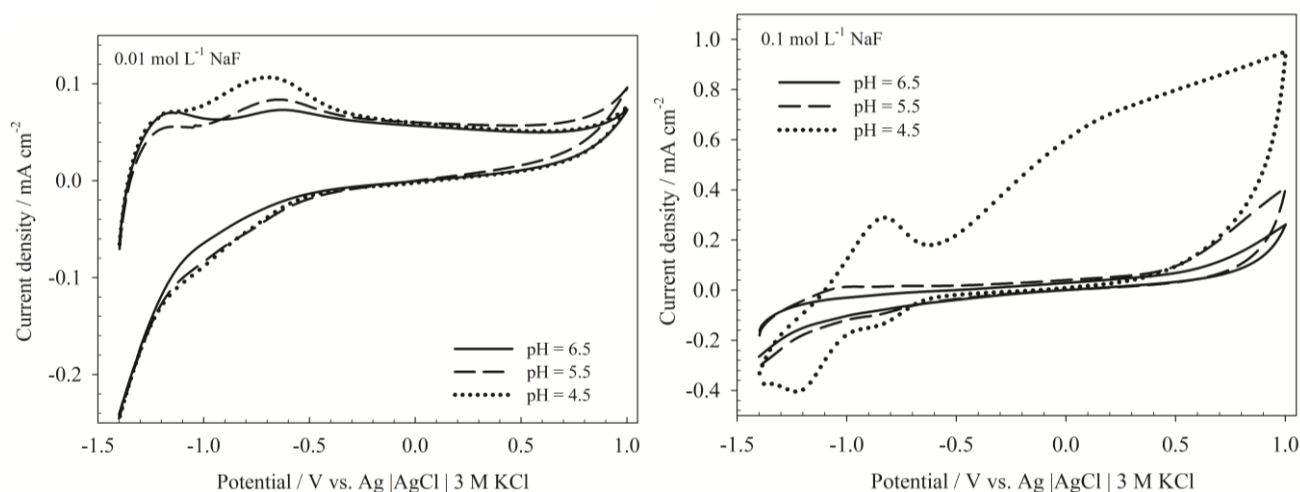
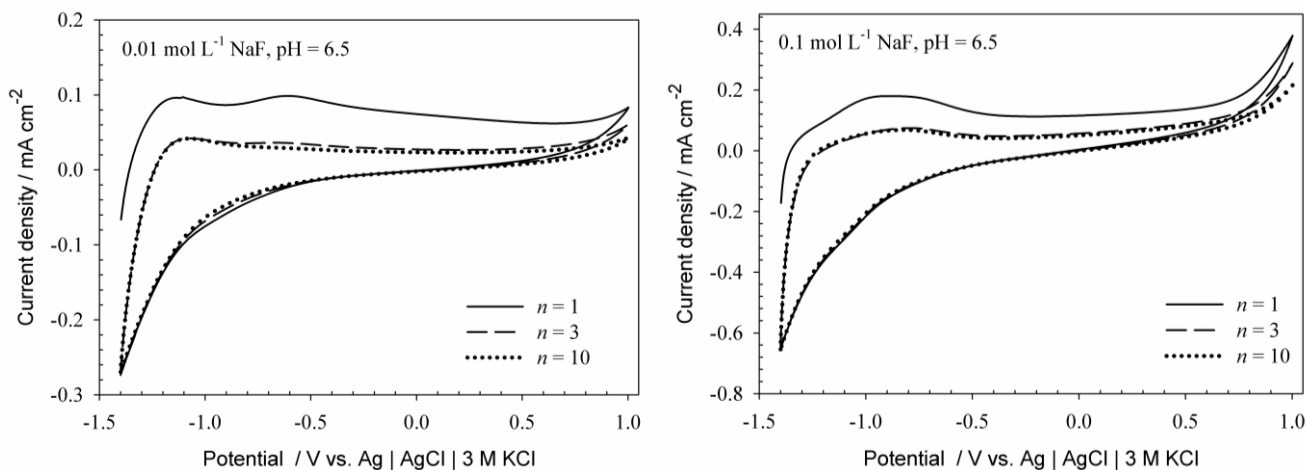


Figure 4. Cyclic voltammograms of iron in 0.01 mol L⁻¹ NaF, pH = 4.5, 5.5, 6.5, $\nu = 100 \text{ mV s}^{-1}$ and 0.1 mol L⁻¹ NaF solutions, pH = 4.5, 5.5, 6.5, $\nu = 20 \text{ mV s}^{-1}$.



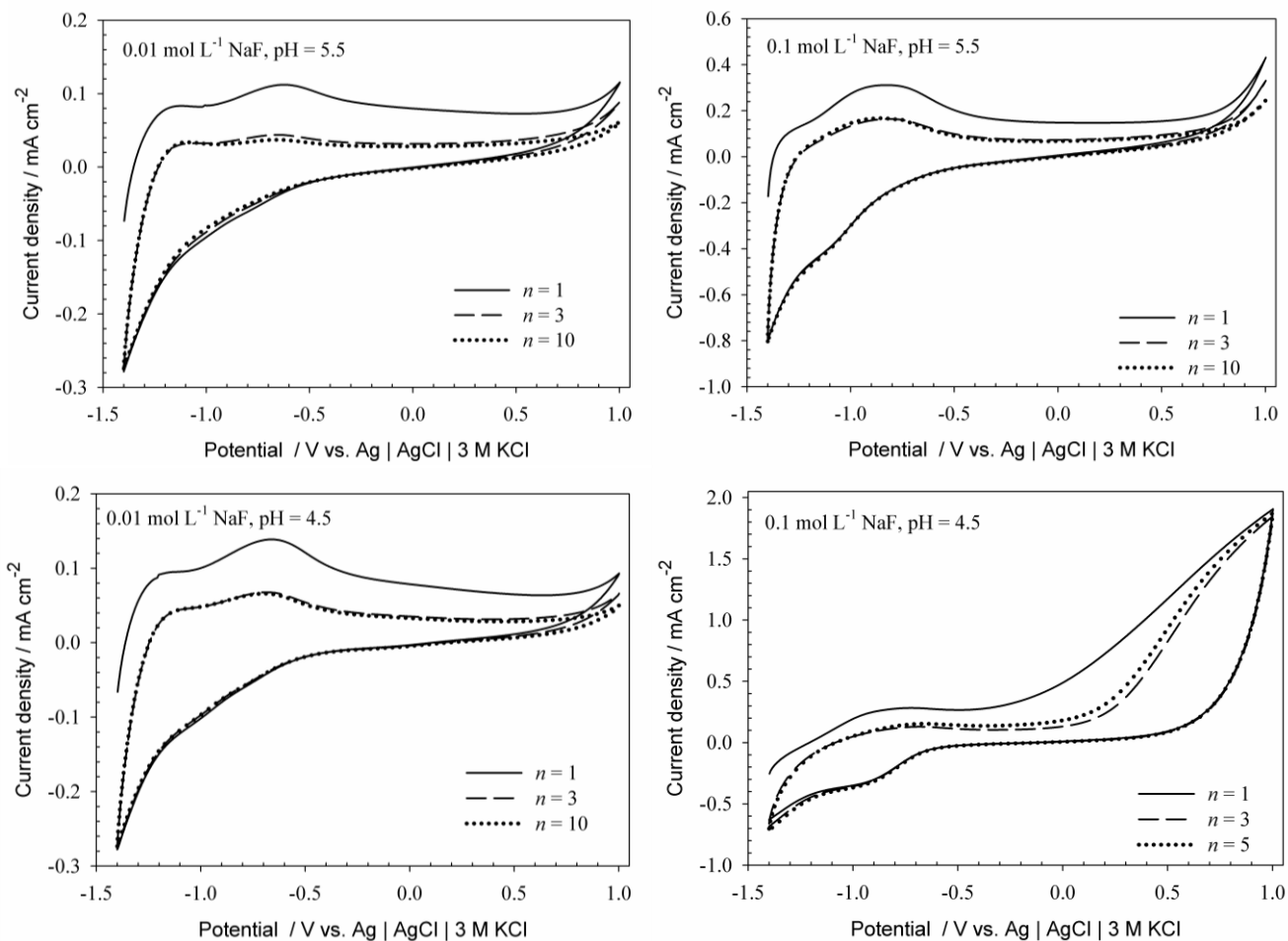


Figure 5. Cyclic voltammograms of continuous cycling of iron electrode with scan rate 130 mV s^{-1} in 0.01 and 0.1 mol L^{-1} NaF, pH = 6.5, 5.5 and 4.5 (number of cycles, n is shown on figure).

Significantly lower current densities of anodic peaks in repeated cycle indicates that in reduction process oxide layer is not reduced completely.

3.2. Electrochemical impedance spectroscopy

A set of impedance spectra recorded with iron electrode in 0.01 and 0.1 mol L^{-1} NaF solutions at open circuit potentials, E_{OCP} (given in Table 3) are presented in Fig. 6 as Nyquist plots.

As can be seen, for all examined solutions, at E_{OCP} the response of the system in the Nyquist complex plane was a capacitive loop which can be correlated with the thickness and the dielectric properties of the oxide film. The diameter of capacitive loop increases with pH value increase and fluoride concentration decrease.

In mathematical analysis of the impedance data a constant phase element (*CPE*) was used instead of an ideal capacitance element to compensate for the non-ideal capacitive response of the interface arising from surface heterogeneities [28, 29]. Its impedance may be defined by: $Z_{\text{CPE}}(\omega) = [Q(j\omega)^n]^{-1}$, where Q is the constant, ω is the angular frequency and n is the *CPE* power with values between 0.5 and 1 [30]. When $n = 1$, the *CPE* describes an ideal capacitor with Q equal to

the capacitance (C). For $0.5 < n < 1$, the CPE describes a distribution of dielectric relaxation times in frequency space, and when $n = 0.5$ the CPE represents a Warburg impedance [31, 32].

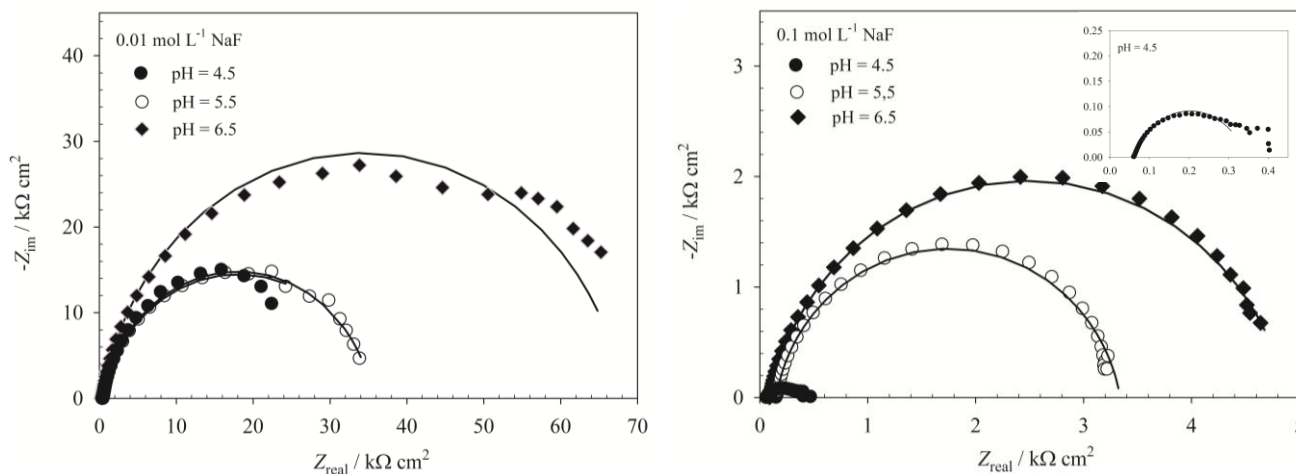


Figure 6. Impedance spectra of iron recorded at the open circuit potential in 0.01 and 0.1 mol L⁻¹ NaF, pH = 4.5, 5.5 and 6.5. The inset: Impedance spectra of iron at the open circuit potential in 0.1 mol L⁻¹ NaF, pH = 4.5.

The equivalent circuit, shown in Fig. 7, was used to fit the experimental data and the resultant EIS parameters are given in Table 3. The equivalent circuit consists of a CPE in the parallel to the resistor R . R_{el} corresponds to the electrolyte resistance which value dependent on fluoride concentration and varied from 20 to 60 $\Omega\text{ cm}^2$ with electrolyte dilution. The value of Q represents the double layer capacitance, C_{dl} , as shown by the high value of the n exponent and R represents the corresponding charge-transfer resistance, R_{ct} . When the pH value increase and the fluoride concentration decrease, the value of the oxide resistance increases and the value of the capacitance decreases. Impedance spectra are recorded on spontaneously formed films at open circuit potential, E_{OCP} . As pH decreases, the open circuit potential values decreases to a value in the active region of iron and less protective films are formed. In 0.1 mol L⁻¹ NaF, pH = 4.5 the oxide film is expected not to have protective properties ($R = 280\ \Omega\text{ cm}^2$) due to the active dissolution of the base metal as suggested by open circuit potential value, $E_{OCP} = -1.129\text{ V}$.



Figure 7. Equivalent electrical circuit used to fit the impedance spectra.

Table 3. Impedance parameters of iron in NaF solutions at open circuit potential.

$c(\text{NaF}) / \text{mol L}^{-1}$	pH	$E_{\text{OCP}} / \text{V}$	$Q \times 10^6 / \Omega^{-1} \text{s}^n \text{cm}^{-2}$	n	$R / \text{k}\Omega \text{cm}^2$
0.01	6.5	-0.240	53.17	0.89	67.97
	5.5	-0.260	62.46	0.89	35.07
	4.5	-0.604	207.20	0.87	40.74
0.1	6.5	-0.250	100.19	0.87	4.80
	5.5	-0.435	100.63	0.89	3.19
	4.5	-1.129	568.78	0.73	0.28

The charge transfer resistance, which corresponds to the diameter of Nyquist plot, is inversely proportional to the corrosion rate. When the overpotential is very small and the electrochemical system is at equilibrium, the expression for the charge transfer resistance can be written as in equation 4 [33]. Corrosion current densities, j_{corr} and corrosion rates, r were calculated using eq. 4 and 5 and presented in Table 4.

$$j_{\text{corr}} = \frac{RT}{zF} \frac{1}{R_{\text{ct}}} \quad (4)$$

$$r = \frac{j_{\text{corr}} M}{zF} \quad (5)$$

Where T is temperature, R is gas constant, F is Faradays constant, z is number of electrons involved, R_{ct} is charge transfer resistance and M is the molar mass of surface oxide.

Table 4. Corrosion current densities and corrosion rates for iron in NaF solutions at open circuit potential.

$c(\text{NaF}) / \text{mol L}^{-1}$	pH	$E_{\text{OCP}} / \text{V}$	$j_{\text{corr}} / \mu\text{A cm}^{-2}$	$r / \mu\text{g cm}^{-2} \text{h}^{-1}$
0.01	6.5	-0.240	0.126	0.25
	5.5	-0.260	0.243	0.48
	4.5	-0.604	0.210	0.42
0.1	6.5	-0.250	1.783	3.54
	5.5	-0.435	2.683	5.33
	4.5	-1.129	30.569	60.69

From the Table 4 it is clear that the increase in fluoride concentration and decrease in pH value markedly increases the corrosion current density and corrosion rate of iron.

4. CONCLUSIONS

The influence of fluoride concentration and pH value on the kinetics of growth and the electrochemical properties of the surface oxide layer on the iron in 0.01 and 0.1 mol L⁻¹ NaF (pH =

4.5, 5.5 and 6.5) was investigated using CV and EIS techniques. The growth of the anodic oxide film, under potentiodynamic conditions, occurs under a low-field migration mechanism. Electric field strength and ionic conductivity through the film were obtained. Thickness of oxide films obtained by analyzing the anodic current curves show that film with better protection properties forms in solution with lower fluoride concentrations and higher pH values (for 0.01 mol L⁻¹ NaF, pH 6.5 $d = 1.37$ nm). Very high value of 39.91 nm for the film thickness in 0.1 mol L⁻¹ NaF, pH 4.5 is pointing on very hydrated layer. Impedance data of iron were analyzed on the bases of proposed electrical equivalent circuit. In all examined electrolytes except in 0.1 mol L⁻¹ NaF, pH 4.5, open circuit potential were in the range of potential where iron passive film is formed and stable. The more protective properties have oxide films in solutions with higher pH and lower fluoride concentration. The investigation showed that iron corrosion rate depends on the fluoride concentration and pH value of the electrolyte. In 0.01 mol L⁻¹ NaF with pH decrease from 6.5 to 4.5 corrosion rate increases from 0.25 $\mu\text{g cm}^{-2} \text{h}^{-1}$ to 0.48 $\mu\text{g cm}^{-2} \text{h}^{-1}$, while in 0.1 mol L⁻¹ NaF this increase was from 3.54 $\mu\text{g cm}^{-2} \text{h}^{-1}$ (pH = 6.5) to 60.69 $\mu\text{g cm}^{-2} \text{h}^{-1}$ (pH = 4.5).

References

1. F-B. Li, D. H. Bremner and A. E. Burgess, *Corros. Sci.*, 41 (1999) 2317
2. P. Marcus, *Corrosion Mechanism in Theory and Practice*, Marcel Dekker Inc., New York, 2002
3. M. Nagayama and M. Cohen, *J. Electrochem. Soc.*, 109 (1962) 781
4. M. Nagayama and M. Cohen, *J. Electrochem. Soc.*, 110 (1963) 670
5. V. Schroeder and T.M. Devine, *J. Electrochem. Soc.*, 146 (1999) 4061
6. M. E. Brett, K. M. Parkin and M. J. Graham, *J. Electrochem. Soc.*, 133 (1986) 2031
7. R.W. Revie, B.G. Baker and J. O'M Bockris, *J. Electrochem. Soc.*, 122 (1975) 1460
8. M. F. Toney, *Phys. Rev. Lett.*, 79 (1997) 4282
9. B. Lochel and H.H. Strehblow, *Electrochim. Acta*, 28 (1983) 565
10. S. J. Ahn, H. S. Kwon and D. D. Macdonald, *J. Electrochem. Soc.*, 152 (2005) B482
11. L. Li, C. Wang, S. Chen, X. Yang, B. Yuan and H. Jia, *Electrochim. Acta*, 53 (2008) 3109
12. T. L. Sudesh, L. Wijesinghe and D. J. Blackwood, *Appl. Surf. Sci.*, 253 (2006) 1006.
13. M. Abdallah, *Mater. Chem. Phys.*, 82 (2003) 786.
14. M. Metikoš-Huković and R. Babić, *Corros. Sci.*, 49 (2007) 3570
15. D. Williams and G.A. Wright, *Electrochim. Acta*, 21 (1976) 1009
16. A.J. Calandra, N.R. de Tacconi, R. Pereiro and A.J. Arvia, *Electrochim. Acta*, 19 (1974) 901
17. R. Babić, M. Metikoš-Huković and Z. Pilić, *Corrosion*, 59 (2003) 890
18. Ž. Petrović, M. Metikoš-Huković, R. Peter and M. Petravić, *Int. J. Electrochem. Sci.*, 7 (2012) 9232
19. S. J. Ahn and H. S. Kwon, *J. Electroanal. Chem.*, 579 (2005) 311
20. Y. F. Cheng, C. Yang and J.L. Luo, *Thin Solid Films*, 416 (2002) 169
21. D.H. Kim, S.S. Kim, H.H. Lee, H.W. Jang, J.W. Kim, M. Tang, K.S. liang, S.K. Sinha and D.Y. Noh, *J. Phys. Chem. B*, 108 (2004) 20213
22. S. J. Ahn and H. S. Kwon, *Electrochim. Acta*, 49 (2004) 3347
23. D.D. Macdonald and M Urquidi – Macdonald, *J. Electrochem. Soc.*, 137 (1990) 2395
24. B. Krishnamurthy, R. E. White and H. J. Ploehn, *Electrochim. Acta*, 47 (2002) 3375
25. E. Sikora and D.D. Macdonald, *J. Electrochem. Soc.*, 147 (2000) 4087

26. D.D. MacDonald, *Pure Appl. Chem.*, 71 (1999) 951
27. S.V. Murphy and D.B. Hibbert, *Phys. Chem. Chem. Phys.*, 1 (1999) 5163
28. J. R. Macdonald, *Impedance spectroscopy, emphasizing solid materials and systems*, Wiley, New York, 1987
29. E. M. A Martini and I. L. Muller, *Corros. Sci.*, 42 (2000) 443
30. U. Rammelt and G. Reinhard, *Electrochim. Acta*, 35 (1990) 1045
31. I. D. Raistrick, D. R. Franceschetti and J. R. Macdonald, in *Impedance Spectroscopy Theory, Experiment, and Application*, 2nd edn, edited by E. Barsoukov & J. R. Macdonald, John Wiley & Sons Inc., Hoboken, New Jersey, 2005
32. M. Metikoš-Huković, Z. Pilić, R. Babić and D. Omanović, *Acta Biomater.*, 2 (2006) 693
33. Application Note, *Basics of Electrochemical Impedance Spectroscopy*, Gamry Instruments, Inc. 2010